Reactive & Functional Polymers 71 (2011) 655–665

Contents lists available at ScienceDirect

Reactive & Functional Polymers

journal homepage: www.elsevier.com/locate/react

Enhanced thermal and surface properties of waterborne UV-curable polycarbonate-based polyurethane (meth)acrylate dispersion by incorporation of polydimethylsiloxane

Hyeon-Deuk Hwang, Hyun-Joong Kim *

Lab. of Adhesion and Bio-Composites, Program in Environmental Materials Science, Seoul National University, Seoul 151-921, Republic of Korea

ARTICLE INFO

Article history:
Received 30 November 2010
Received in revised form 24 February 2011
Accepted 4 March 2011
Available online 12 March 2011

Keywords:
UV-curing
Polyurethane
Polycarbonate diol
Polydimethylsiloxane
Surface free energy

ABSTRACT

Hydroxy-terminated polydimethylsiloxane (PDMS) was incorporated into the soft segments of UV-curable polycarbonate-based polyurethane (meth)acrylate dispersions to improve the thermal property and surface property. 2-Hydroxymethacylate or pentaerythritol tri-acrylate was end-capped with or without PDMS to confirm the effect of the functionality of the end-capping group on the properties. Owing to the hydrophobicity of siloxane, the cured coating films containing PDMS had low surface free energy, and higher thermal degradation temperature. The functionality of the end-capping group had a slight effect on the surface and thermal properties. The UV-curing rate and final conversion depended strongly on the functionality. The glass transition temperature and the tensile strength of the cured films were increased by incorporating PDMS or increasing the functionality. Therefore, the weaknesses of waterborne UV-curable coatings can be alleviated by the incorporation of PDMS and high functionality.

1. Introduction

Owing to increasing needs and environmental concerns, the development and trends of coatings have focused on more environmental-friendly coating with lower cost but without a loss of performance. Various types of coatings technology have been developed to fulfill these requirements. For example, high-solid coatings contain a low content of volatile organic solvents less than 30% and waterborne coatings employ water as a medium instead of harmful organic solvents. Other methods are solvent-free systems such as radiation (UV/EB) curing, two-components system or powder coatings [1,2].

Among these technologies, UV-curable waterborne technology has come to occupy an important position. It is a merging technology that combines waterborne and UV-curing systems to overcome drawbacks of each other and combine their advantages. The drawbacks of UV-curing systems, such as volatility, toxicity, flammability, and odor due to unreacted low molecular weight reactive diluents, can be eliminated due to high molecular weight of the dispersion. In dispersions, it is possible to obtain the low viscosity necessary for spray applications independent of the molecular weight because the viscosity of dispersions depends only on the particle size and concentration. High volume shrinkage problems during the UV-curing process can be reduced because the physically dried films after water evaporation, in spite of not crosslinking, have resistance to the internal stress and make a tack-free surface. In addition, the weak properties of waterborne systems such as low gloss, water repellency, scratch and chemical resistance can be improved with a crosslinked structure formed by UV-curing [3–6].

There are three designs for waterborne UV-curable systems: emulsions, water-soluble resins, and dispersions. Hydrophobic UV-curable systems can be emulsified, dissolved or dispersed in water with the aid of a protective colloid, external emulsifier or by structural modifications [7,8]. However, emulsion or water-soluble systems have some disadvantages because they require a strong shear force to disperse the polymer, which results in coarse particles as well as poor dispersion stability and film properties [9].

In contrast, polyurethane dispersions are made by incorporating hydrophilic or ionic groups, which act as internal emulsifiers or self-emulsifier, into the backbone of resins. In this method, the dispersion can be made under mild conditions and produced as a finer particle size. As a result, the dispersion stability and film properties can be improved [9]. Generally, polyurethane dispersions are used because polyurethane is a unique class of polymer that can obtain various properties by the selection of different components and have wide applications in a number of different industrial sector such as coatings, foams, adhesives, sealants, synthetic leathers, membranes, elastomers as well as many biomedical applications [10].

* Corresponding author. Tel.: +82 2 880 4784; fax: +82 2 873 2318.
E-mail address: hjokim@snu.ac.kr (H.-J. Kim).

1381-5148/$ - see front matter © 2011 Elsevier Ltd. All rights reserved.
doi:10.1016/j.reactfunctpolym.2011.03.004

Polydimethylsiloxane (PDMS) is used in range of applications owing to its unique features, such as high thermal and oxidative stability, weather and chemical resistance, and low surface tension. However, PDMS has disadvantages, such as relatively poor mechanical characteristics resulting from its low-temperature flexibility based on a low glass transition temperature (−123 °C) [11–13]. Another shortcoming is its incompatibility with organic polymers arising from the non-polar nature of the siloxanes based on its very low solubility parameter (δ = 14.9 $J^{1/2}$ $cm^{-3/2}$) compared to other polymers (δ = 17.6–28.6 $J^{1/2}$ $cm^{-3/2}$) [3,14].

In this study, waterborne polyurethane (meth)acrylate dispersions were modified with a hydroxy-terminated PDMS to improve the thermal stability and surface properties. The incorporation of PDMS into the soft segments of the polyurethane backbone was carried out by a reaction between NCO and OH groups in the diisocyanates and hydroxy-terminated PDMS, respectively. In this method, the flexible siloxane chain can be tailored easily onto the surface without resistance during the UV-curing process. Generally, polysiloxanes are quite flexible and have good low temperature properties but poor physical–mechanical properties [15,16]. A lower molecular weight of PDMS (550 g/mol) compared to that of polycarbonate diol (PCDL, 800 g/mol) was used to compensate low physical–mechanical properties of PDMS.

A PCDL was used as a polyol to achieve better mechanical properties for surface coatings applications. In particular, linear aliphatic polycarbonates are used as both binders in high-quality polyurethane coatings and in the production of polyurethane binders or polyurethane dispersions [17,18]. The PCDL used in this study were C5/C6 copolymers, which were prepared from 1,6-hexanediol, 1,5-pendanediol and ethylene carbonate (Asahi Kasei Chemicals Corp.). The C5/C6 copolymer has lower viscosity, better weather stability and very good resistance to hydrolysis [19–21].

In first step of the synthesis process, C5/C6 copolymers of polycarbonate were reacted with Isophorone diisocyanate to produce NCO-terminated intermediates. Hydroxy-terminated PDMS was incorporated by a reaction with the NCO-terminated intermediates. Dimethylolpropionic acid (carboxyl groups) was incorporated into the polyurethane main chain for self-emulsification. To confirm the effect of the functionality of the end-capping group on the properties, 2-hydroxymethacylate or pentaerythritol tri-acrylate was end-capped with or without a PDMS system. The synthesized resins were then neutralized with triethyl amine (base) and dispersed in an aqueous medium with a radical type photo-initiator. The UV-curing behaviors and characterization were evaluated after the synthesis and dispersion process.

2. Experimental

2.1. Materials

Table 1 lists the chemical structures and properties of the raw materials used for synthesis. A polycarbonate diol (PCDL, Asahi Kasei Chemicals Corp.) and dimethylol propionic acid (DMPA, Across Organics) were dried and degassed at 80 °C under vacuum for 6 h. A hydroxy-terminated polydimethylsiloxane (PDMS, Sigma Aldrich) was used as received. Isophorone diisocyanate (IPDI, Bayer Material Science) and triethyl amine (TEA, Samchun Pure Chemical) were dried using a 4 Å molecular sieve prior to use. Either 2-hydroxyethylmethacrylate (2-HEMA, Junsei Chemicals) or pentaerythritol tri-acrylate (PETA, Sigma Aldrich) was used as the end-capping agent without further purification. A radical type photo-initiator (Irgacure 500, Ciba Specialty Chemicals) was used as received. All samples used in the synthesis were extra pure or regent grade.

2.2. Synthesis of UV-curable PDMS-modified polycarbonate-based polyurethane dispersion

Fig. 1 and Table 2 show the synthesis process and formulation of UV-curable PDMS-modified polycarbonate-based polyurethane dispersions, respectively. At each step, the reaction time was determined by observing the changes of the FT-IR peak at 2265 cm^{-1} (NCO peak) which decreased with the progression of the polyurethane reaction. Initially, IPDI was charged into a dried 300 ml round bottom flask equipped with a four-necked separable flask with a mechanical stirrer, thermometer and condenser with a drying tube and N_2 inlet. The temperature was increased to 70 °C using a constant temperature heating mantle with constant stirring. Then, PCDL with some of the catalyst (dibutyltin dilaurate, approximately 500 ppm) were added dropwise over a 2 h period and maintained for further 1 h. A hydroxy-terminated PDMS was dropped and reacted for 2 h. DMPA as an ionic group was dropped for 1.5 h and reacted for 1 h. The reaction temperature cooled to 50 °C, and 2-HEMA or PETA was added dropwise over a 2 h period and reacted for 3 h until the NCO peak had almost disappeared. After cooling to ambient temperature, TEA was then added as a neutralizing agent and stirred for a further 0.5 h. In the final step, water was mixed and stirred at 3000 rpm for 1 h. Irgacure 500 (3 wt%) was then added as an radical type photo-initiator for UV-curing initiation.

2.3. Coating and curing process

PDMS-modified polycarbonate-based polyurethane dispersions were applied onto glass plates using an applicator at a 40 μm thickness and dried in an oven at 80 °C for 5 min. The tack-free dried films were cured by passing under a conveyor type UV-curing machine equipped with medium-pressure mercury UV-lamps (100 W/cm, main wave length: 365 nm). The irradiated UV-dose measured by an UV radiometer (IL 390C Light Bug, International Light Inc.) was 3000 mJ/cm^2 to measure contact angle. To prepare free standing film samples for measuring dynamic mechanical analysis, tensile strength and thermogravimetric analysis, the dispersions were cast on an aluminum pan and dried at ambient temperature for 1 day and then, in an oven at 60 °C for 1 day. The thickness of fully dried film was 500–600 μm. The dried films were then cured using a conveyor type UV-curing machine at a UV-dose of 3000 mJ/cm^2.

2.4. Curing behavior and characterization properties

2.4.1. Average particle size

An electrophoretic light scattering spectrophotometer (ELS-8000, Otsuka Electronics) was used to measure the average particle size of the dispersion at ambient temperature. The dispersion was diluted with deionized water to approximately 1% and the measurements were carried out twice.

2.4.2. Monitoring synthesis process and UV-curing behavior by Fourier transform infrared (FT-IR) spectroscopy

FT-IR spectroscopy was used for two purposes, monitor the polyurethane reaction and evaluate the UV-curing behavior. Polyurethane synthesis was controlled by monitoring the disappearance of the characteristic peaks of the NCO groups (2265 cm^{-1}). The IR spectra were recorded on a JASCO FT/IR-6100 (Japan) equipped with a Miracle accessory, which is a type of attenuated total reflectance made from ZnSe. The FT-IR spectra were recorded from 4000 to 650 cm^{-1} with a 4 cm^{-1} resolution.

Table 1
Raw materials used for the synthesis of UV-curable PDMS-modified polycarbonate-based polyurethane (meth)acrylate dispersions.

Function	Materials	Abbreviation	Chemical structure	Molecular weight (g/mol)	Supplier
Polyol	Polycarbonate diol	PCDL	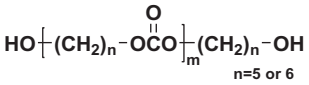 n=5 or 6	800	Asahi Kasei Chemicals Corp.
Isocyanate	Isophorone diisocyanate	IPDI	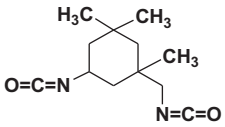	222	Bayer Material Science
Surface energy modifier	Polydimethylsiloxane	PDMS	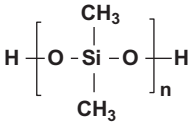	550	Sigma Aldrich
Ionomer	Dimethylol propionic acid	DMPA	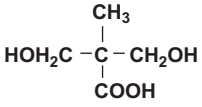	134	Acros Organics
End-capping agent	2-Hydroxyethylmethacrylate	2-HEMA	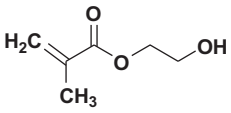	130	Samchum Chemicals
	Pentaerythritol tri-acrylate	PETA	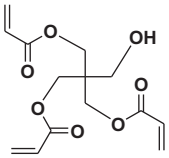	298	Sigma Aldrich
Neutralizing agent	Triethylamine	TEA	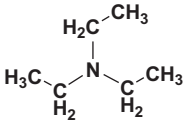	101	Samchum Chemicals
Catalyst	Dibutyltin dilaurate	DBTDL	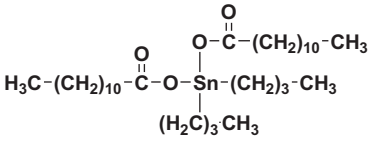	631.6	Alfa Sesar
Photo-initiator	Irgacure 500	I500	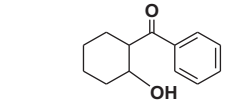 1-hydroxy-cyclohexyl-phenyl-ketone (50 wt%)	204	Ciba Specialty Chemicals
			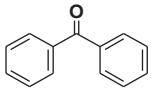 benzophenone (50 wt%)	182	

2.4.3. UV-curing behavior by photo differential scanning calorimetry (photo-DSC)

To examine the UV-curing behavior, the photo-DSC experiments were carried out using a DSC (Q-1000, TA Instruments) equipped with a photocalorimetric accessory (Novacure 2100), which used the light from a 100 W medium-pressure mercury lamp (main wave length: 250–650 nm). The light intensity was determined by placing an empty DSC pan on the sample cell. The UV-light intensity at the sample was 50 mW/cm^2. The weight of the sample was approximately 2 mg and the sample was placed in an open aluminum DSC pan. Before UV-curing, the water contained in the samples was evaporated at 50 °C for 10 min. The measurements were carried out at 30 °C in flowing N_2 gas at 50 ml/min.

2.4.4. Surface free energy

To evaluate the surface free energy of the UV-cured films, the static contact angles were measured using a contact angle analyzer (SEO 300A, Surface & Electro-Optics Corp.). The temperature and relative humidity were 23 ± 2 °C and 50 ± 3%, respectively. The equilibrium contact angle is defined as the angle between the solid surface and a tangent, drawn on the drop-surface, passing through the triple-point atmosphere-liquid–solid [22]. The relationship between these three interfacial tensions is given by Young's equation as the following equation:

$$\cos\theta = \frac{\gamma_{solid/vapor} - \gamma_{solid/liquid}}{\gamma_{liquid/vapor}} \quad (1)$$

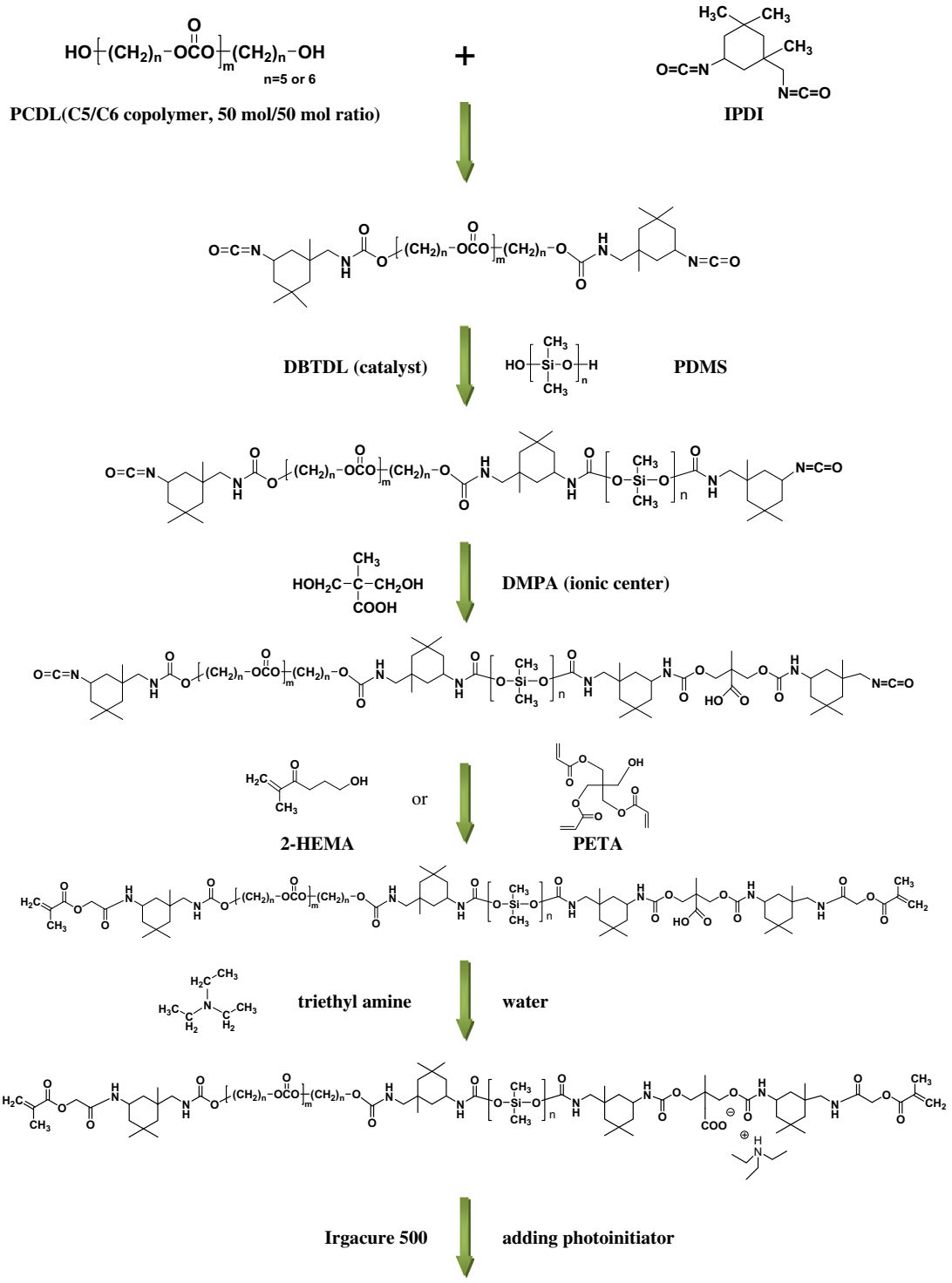

Fig. 1. Synthesis process of UV-curable PDMS-modified polycarbonate-based polyurethane (meth)acrylate dispersions.

2.4.5. Viscoelastic properties by dynamic mechanical analysis (DMA)

The viscoelastic properties of the UV-cured films were analyzed using a dynamic mechanical analysis instrument (Q800, TA Instruments). The samples were prepared as rectangular specimens, 12 mm in length, 6.6 mm in width and 0.5 mm in thickness. The measurements were taken in tension mode at a frequency of 1 Hz and strain of 0.1%. The temperature ranged from −100 °C to 150 °C at a scanning rate of 2 °C/min. The storage modulus (E'), loss modulus (E'') and loss factor ($\tan\delta$) of the cured films were measured as a function of temperature.

2.4.6. Tensile strength

The tensile strength was measured using a Universal Testing Machine (Zwick Corp.) at ambient temperature with a crosshead speed of 100 mm/min. The UV-cured films were prepared as rectangular specimens, 20 mm in length (span length), 6.6 mm in

Table 2
Formulations used for the synthesis of UV-curable PDMS-modified polycarbonate-based polyurethane (meth)acrylate dispersions (units in mole).

Sample	PCDL	Isocyanate IPDI	End-capping agent		PDMS	Ionomer DMPA	Neutralizing agent TEA
	800		2-HEMA	PETA			
WPCU-L800-1MA	0.185	0.444	0.185			0.093	0.093
WPCU-L800-3A	0.185	0.444		0.185		0.093	0.093
WPCU-L800-Si-1MA	0.139	0.444	0.185		0.046	0.093	0.093
WPCU-L800-Si-3A	0.139	0.444		0.185	0.046	0.093	0.093

width and 0.5 mm in thickness. Five measurements were taken with the mean value used for further analysis.

2.4.7. Thermogravimetric analysis

The thermal stability and decomposition profiles of the UV-cured films were measured using a thermogravimetric analyzer (Q-5000 IR, TA Instruments). 5 milligram of the UV-cured sample was loaded into a ceramic pan, and heated from 30 °C to 600 °C at a constant heating rate of 10 °C/min in an inert nitrogen atmosphere. The balanced and sample purge flows were 10.0 mL/min and 25.0 mL/min, respectively.

2.4.8. Wide angle X-ray diffraction

Wide angle X-ray diffraction (WAXD, D8-Advance, Bruker Miller Co.) analysis was carried out to investigate the state of the UV-cured films. Monochromatic Cu Kα radiation was used at the rate of 2° 2θ/min in the range of 5–50° 2θ.

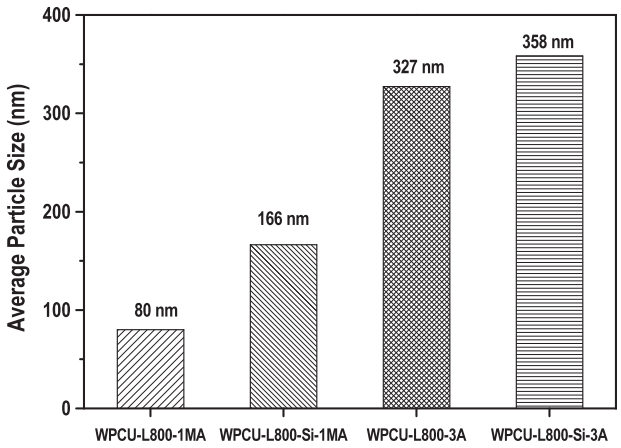

Fig. 2. Average particle size of UV-curable PDMS-modified polycarbonate-based polyurethane (meth)acrylate dispersions.

3. Results and discussion

3.1. Average particle size of dispersion

Several factors affect the particle size of the dispersion. The particle size of dispersion increases with increasing viscosity of the dispersant, which is related to the prepolymer molecular weight, ionic group content and molecular structure. The location of the ionic group and main chain flexibility also affect the particle size. For example, dispersion with ionic groups in the soft segment has a much smaller particle size and greater viscosity than those with ionic groups in the hard segment. This is because ionic groups can easily tailor the surface during dispersion owing to the easier conformation change in the soft segment [23–25]. Another factor is the property of the materials formulated or incorporated into the dispersion. The hydrophilicity of a dispersion can be changed using various functional materials, such as PDMS [16,26], fluorine [27], clay [28], and PDMS with fluorine [29], which determines the particle size of the dispersion.

Fig. 2 shows the effects of the functionality and PDMS on the particle size of the dispersions. The average particle size of WPCU-L800-3A (327 nm) was much larger than that of WPCU-L800-1MA (80 nm). The hydrophobicity of WPCU-L800-3A increased due to their bulky tri-acrylate groups on each end of the chain, which produced a much larger particle size than WPCU-L800-1MA with smaller mono-methacrylate groups on each end of the chain [13]. The average particle sizes of WPCU-L800-Si-1MA (166 nm) and WPCU-L800-Si-3A (358 nm) were larger than WPCU-L800–1MA (80 nm) and WPCU-L800-3A (327 nm), respectively. The incorporation of PDMS into the polyurethane main chain can increase the particle size regardless of the functionality of the end-capping due to the hydrophobicity of the PDMS chains [3]. Increasing the functionality has a stronger effect on the particle size than the incorporation of PDMS.

3.2. UV-curing kinetics by photo-DSC

The kinetics of the UV-curing reaction is a useful information for applying UV technology to each application area. However, monitoring the UV-curing behavior is very difficult owing to its extremely rapid curing speed. In this study, the UV-curing behavior was measured by photo-DSC measurements, which is a convenient method for evaluating the reactivity and measuring the kinetics of the *in situ* UV-curing reaction.

Fig. 3 shows the isothermal UV-curing heat enthalpy and conversion profiles of UV-curable PDMS-modified polyurethane dispersion. The heat flow (cal/g s) plotted in Fig. 3a can only be acquired by photo-DSC measurements and advanced analysis (Fig. 3b–d) are the results of further calculations. The reaction enthalpy was calculated by integrating the area under the exothermic peak using the following equation [30,31]:

$$\alpha = \frac{\Delta H_t}{\Delta H_0^{theor}} \tag{2}$$

where ΔH_t is the reaction heat enthalpy released at time t and ΔH_0^{theor} is the theoretical heat enthalpy for complete conversion. ΔH_0^{theor} of acrylate and methacrylate are 86 kJ/mol (20.6 kcal/mol) and 54.4 kJ/mol (13.1 kcal/mol), respectively [32,33]. The heat of polymerization of each sample (ΔH_0^{theor} (sample)) was calculated using the following equation:

$$\Delta H_0^{theor}(sample) = \frac{\Delta H_0^{theor}(acrylate)/\Delta H_0^{theor}(methacrylate)}{MW^{theor}} \times Functionality \tag{3}$$

where MW^{theor} is the theoretical molecular weight of the repeating unit. Table 3 lists the calculated results of all samples. The rate of polymerization (R_p) is related directly to heat flow (dH/dt) using the following equation [30,31]:

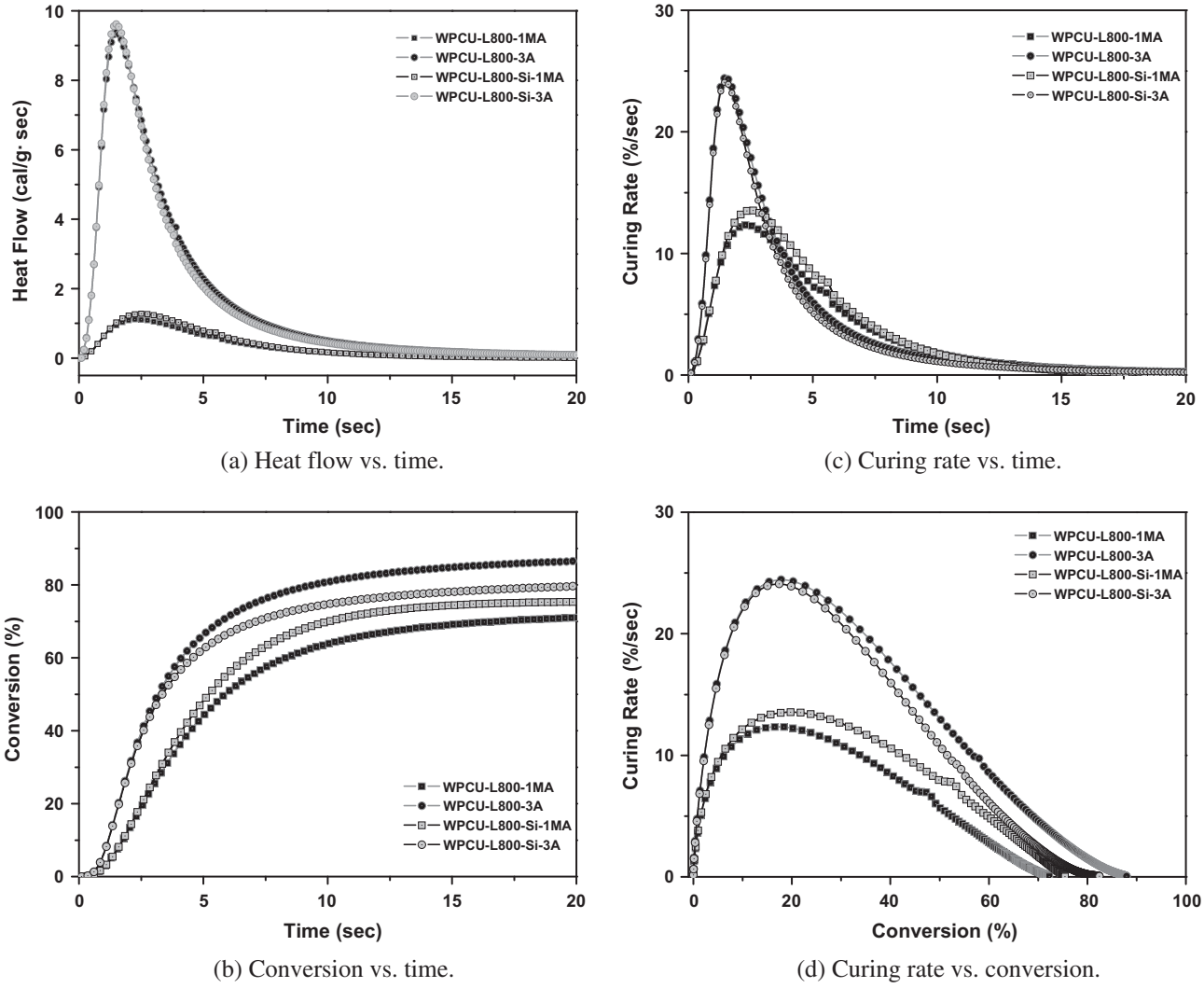

Fig. 3. Isothermal UV-curing heat enthalpy and conversion profiles of UV-curable PDMS-modified polycarbonate-based polyurethane (meth)acrylate dispersions by photo-DSC. (a) Heat flow vs. time, (b) conversion vs. time, (c) conversion rate vs. time, and (d) conversion rate vs. conversion.

$$R_p = \frac{d\alpha}{dt} = \frac{(dH/dt)}{\Delta H_0^{theor}} \quad (4)$$

where $d\alpha/dt$ is the conversion rate or polymerization rate, δH_0^{theor} is the total exothermic heat of reaction and dH/dt is the measured heat flow at a constant temperature.

There are several factors that determine the UV-curing behavior including UV-light intensity and UV-dose, species and content of photo-initiator, reaction temperature, and the reactivity of functional groups [30]. Fig. 3a and Table 4 show the exothermic heat flows during the UV-curing. At the beginning of the reaction, the early onset of auto-acceleration by the activation of radicals occurred as a steep increase, which was followed by auto-deceleration as indicated in the rapid dropping curves. A difference in activity between the tri-acrylate end-capping and mono-methacrylate was observed. The curing rate and conversion of tri-acrylate functionality were much higher than those of the other samples with mono-methacrylate functionality.

The conversion of each sample was calculated using Eqs. (2) and (3) as shown in Fig. 3b. The final conversion was in the following order: WPCU-L800-1MA (72.3%) < WPCU-L800-Si-1MA (75.5%) < WPCU-L800-Si-3A (81.5%) < WPCU-L800-3A (88.1%). Fig. 3c and Table 4 show the curing rate as function of time and the peak time with the maximum curing rate. Fig. 3d shows plots of the curing rate versus conversion.

The curing rate peak appeared first at 1.50 s (WPCU-L800-3A) and 1.55 s (WPCU-L800-Si-3A), the maximum curing rate was 24.5%/sec (WPCU-L800-3A) and 24.1%/s (WPCU-L800-Si-3A),

Table 3
Calculated theoretical reaction enthalpy of the UV-curable PDMS-modified polycarbonate-based polyurethane (meth)acrylate dispersions.

Samples	Theoretical molecular weight of repeating unit	Functionality	Theoretical reaction enthalpy			
			kJ/mol	J/g	kcal/mol	cal/g
WPCU-L800-1MA	2883.6	2 methacrylate	108.8	37.7	26.2	9.0
WPCU-L800-3A	3219.9	6 acrylate	516.0	160.3	123.6	38.3
WPCU-L800-Si-1MA	2758.6	2 methacrylate	108.8	39.4	26.2	9.4
WPCU-L800-Si-3A	3094.9	6 acrylate	516.0	166.7	26.2	39.8

Table 4
Peak time of the curing rate, maximum curing rate, and final conversion of UV-curable PDMS-modified polycarbonate-based polyurethane (meth)acrylate dispersions by photo-DSC.

Samples	Peak time of curing rate (s)	Maximum curing rate (%/s)	Final conversion (%)
WPCU-L800-1MA	2.35	12.3	72.3
WPCU-L800-3A	1.50	24.5	88.1
WPCU-L800-Si-1MA	2.50	13.6	75.5
WPCU-L800-Si-3A	1.55	24.1	81.5

which was much higher than the mono-methacrylate end-capped samples. Therefore, the curing rate and conversion increased with increasing the functionality of the end-capping groups, because coatings with higher functionality are easily activated and continued the reaction.

On the other hand, the effect of PDMS incorporation was different from that of the functionality of end-capping. The curing rate and final conversion of PDMS with mono-methacrylate increased slightly, but those of PDMS with tri-acrylate decreased slightly. The former was affected more by the chain flexibility of PDMS, and the latter was affected more by the steric hindrance caused by PDMS.

3.3. Surface free energy

The first quantitative calculation the surface free energy was determined from contact angles based on Young's equation. In this study, the three liquids method was employed which was suggested by Good [34] and has been widely used to study the surface free energy of polymeric coating films. The test liquids used in this study were distilled water, formamide and diiodomethane and their surface tension parameters are listed in Table 5. From these contact angles of liquids, surface free energy can be calculated by using the following equations:

$$\gamma_{LV}(1+\cos\theta_1) = 2\sqrt{\gamma_S^{LW}\gamma_{LV1}^{LW}} + \sqrt{\gamma_S^{+}\gamma_{LV1}^{-}} + \sqrt{\gamma_S^{-}\gamma_{LV1}^{+}}$$
$$\gamma_{LV}(1+\cos\theta_2) = 2\sqrt{\gamma_S^{LW}\gamma_{LV2}^{LW}} + \sqrt{\gamma_S^{+}\gamma_{LV2}^{-}} + \sqrt{\gamma_S^{-}\gamma_{LV2}^{+}}$$
$$\gamma_{LV}(1+\cos\theta_3) = 2\sqrt{\gamma_S^{LW}\gamma_{LV3}^{LW}} + \sqrt{\gamma_S^{+}\gamma_{LV3}^{-}} + \sqrt{\gamma_S^{-}\gamma_{LV3}^{+}}$$

$$\gamma = \gamma_S^{LW} + \gamma_S^{AB} = \gamma_S^{LW} + 2\sqrt{\gamma_S^{+}\gamma_s^{-}} \tag{5}$$

where *LW* and *AB* represent the Lifshitz–van der Waals and the acid-basic interaction, respectively, γ is the surface free energy contributed by Lifshitz–van der Walls (γ^{LW}) and acid–base interaction (γ^{AB}). γ^{+} and γ^{-} are the Lewis acid parameter and the Lewis base parameter of surface free energy, respectively. In same manner,

Table 5
Parameters of testing liquids for the calculation of surface free energy by three liquid method.

Parameters	Liquid (mN/m)		
	Water (H_2O)	Formamide ($HCONH_2$)	Diiodomethane (CH_2I_2)
Surface free energy (γ)	72.80	58.00	50.80
Dispersive (γ^{LW})	21.80	39.00	50.80
Polar (γ^{AB})	51.00	19.00	0
Acid (γ^{+})	25.50	2.28	0
Base (γ^{-})	25.50	39.60	0

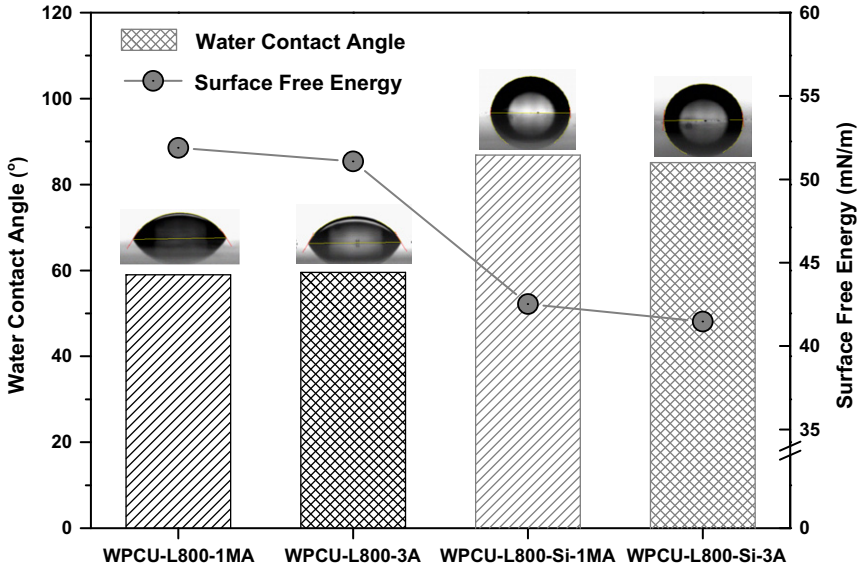

Fig. 4. Water contact angles and surface free energy of the UV-cured film of PDMS-modified polycarbonate-based polyurethane (meth)acrylate dispersions.

Table 6
Contact angle and surface free energy of the UV-cured film of PDMS-modified polycarbonate-based polyurethane (meth)acrylate dispersions.

Samples	Contact angle (°)			Surface free energy (mN/m)		
	Water	Formamide	Diiodomethane	γ_s	γ_s^{LW}	γ_s^{AB}
WPCU-L800-1MA	59.0	36.2	21.6	51.9	47.3	4.6
WPCU-L800-3A	59.5	39.9	13.1	51.1	49.5	1.6
WPCU-L800-Si-1MA	86.9	56.7	36.4	42.5	41.4	1.2
WPCU-L800-Si-3A	85.1	53.3	40.3	41.5	39.5	2.0

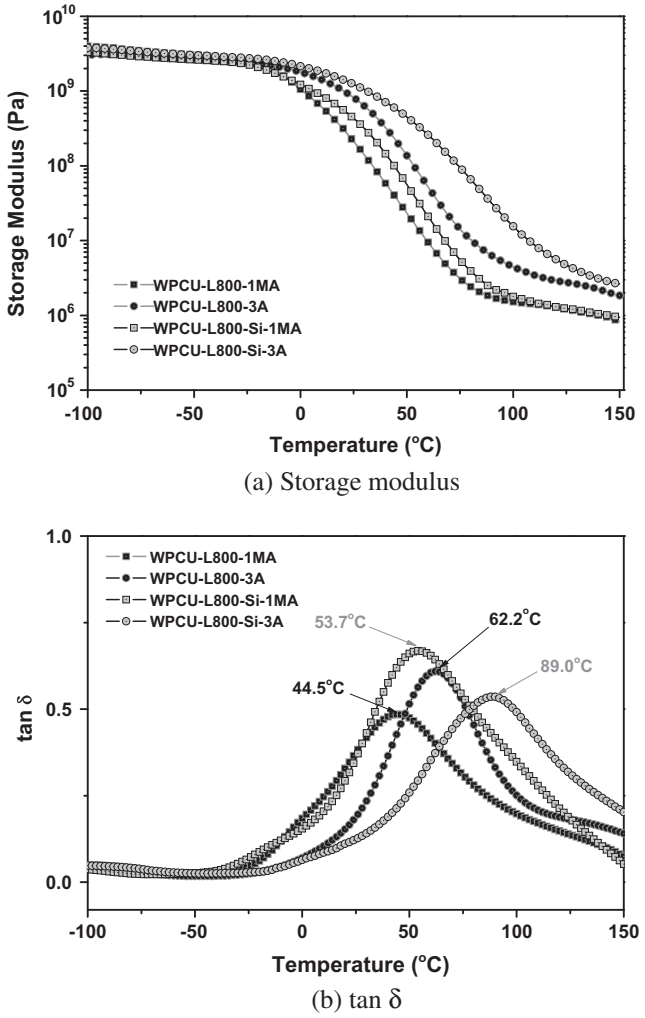

Fig. 5. Viscoelastic properties of the UV-cured film of PDMS-modified polycarbonate-based polyurethane (meth)acrylate dispersions. (a) Storage modulus, (b) tan δ.

γ_{LV} is the surface tension of the liquid in equilibrium with its own vapor and the subscripts 1, 2 and 3 represent liquids 1, 2 and 3, respectively. γ_{LV}^{LW}, γ_{LV}^{+}, γ_{LV}^{-}, γ_{LV} are all available, the surface tension g could be obtained by solving the above Eq. (5) [22,35–37].

Contact angle and surface free energy of UV-cured films are shown in Fig. 4 and Table 6. It was clearly observed that contact angles of all three liquids increased with the incorporation of PDMS. In particular, water contact angle of cured films containing PDMS (WPCU-L800-Si-1MA and WPCU-L800-Si-3A) increased approximately 25° compared to cured film without PDMS. As a result, surface free energy also decreased due to the surface activity of hydrophobic siloxane incorporated into the soft segment [38]. However, a small difference of contact angle was observed between the cured films with different functionality. These results show that surface free energy depends strongly on the hydrophobicity of coating surface rather than the functionality or crosslink density.

3.4. Viscoelastic properties

DMA is a convenient and widely used method for examining the thermal, mechanical and viscoelastic properties of UV-cured polymeric materials. Changes in the loss or storage modulus, glass transition temperature (T_g), crosslink density and relaxation behavior of the polymeric materials can be acquired by DMA. In the case of urethane polymers, the relationship between the structure and property can be analyzed by examining the ratios and organization, as well as the interaction between the hard and soft segments, which have a dominant influence on the physical and mechanical properties [39].

Fig. 5 shows the influence of functionality of the end-capping groups and PDMS on the viscoelastic properties. The storage modulus (E') decreased rapidly near T_g due to vibrations of the molecular segments, as shown in Fig. 5a. The decrease in storage modulus continued until its rubbery plateau, and further progress to the flowing region was restricted by the chemical crosslinks. Fig. 5b shows tan δ curves and T_g. Generally, T_g is determined from the temperature associated with the peak magnitude of the loss factor (tan δ) [40].

The crosslink density, which is related closely to the other physical properties, is expressed as v (mol/g; $0 \leqslant v$) or the degree of crosslinking (X_c; $0 \leqslant X_c \leqslant 1$). The theoretical molecular weight between crosslinks (M_c) is a reciprocal of X_c, which is can be calculated using the following equation:

$$M_c = \frac{M_0}{pf_0 - 2} \tag{6}$$

where M_0 is the average molecular weight, f_0 is the average functionality, and p is the fraction of converted groups ($p \leqslant 1$). Table 7

Table 7
Calculated theoretical molecular weight between the crosslinks (M_c) and degree of crosslinking (X_c) of the UV-cured film using the final conversion measured by FT-IR and photo-DSC, actual M_c and X_c measured by DMA.

Samples	Theoretical *MW*	Functionality	Theoretical M_c and X_c by photo-DSC			Actual M_c and X_c by DMA	
			Final conversion (%)	M_c (g/mol)	X_c ($\times 10^3$)	M_c (g/mol)	X_c ($\times 10^3$)
WPCU-L800-1MA	2884	4 (2 double bond)	72.3	3277	0.305	2708	0.369
WPCU-L800-3A	3220	12 (6 double bond)	88.1	376	2.662	784	1.276
WPCU-L800-Si-1MA	2759	4 (2 double bond)	75.5	2705	0.370	2243	0.446
WPCU-L800-Si-3A	3095	12 (6 double bond)	81.5	398	2.514	720	1.389

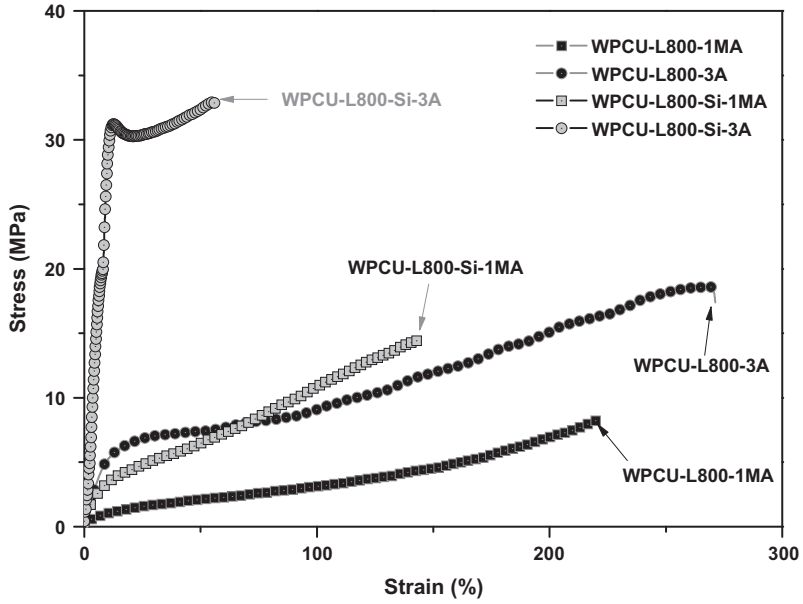

(a) Strain-stress curve

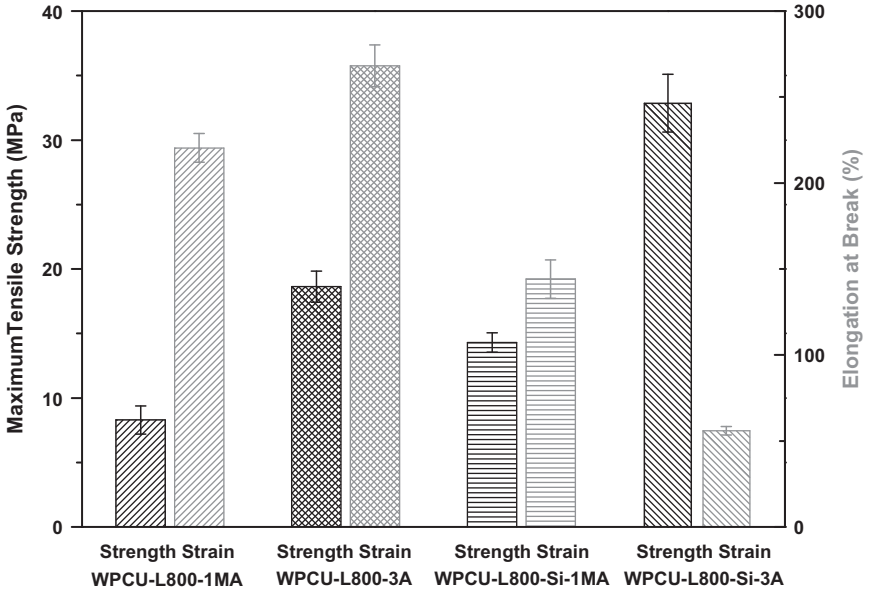

(b) Maximum tensile strength and elongation at break

Fig. 6. Tensile behavior of the UV-cured film of PDMS-modified polycarbonate-based polyurethane (meth)acrylate dispersions. (a) Strain–stress curves, (b) maximum tensile strength and elongation at break.

lists the calculated results [7]. Both the final conversions (p) by photo-DSC measurements were used to calculate the theoretical M_c and X_c. The crosslink density also can be determined experimentally by DMA based on the theory of rubber elasticity using the following equation [24,41]:

$$G_N^0 = \frac{\rho RT}{M_c} \tag{7}$$

where G_N^0 is the rubbery plateau modulus, ρ is the density, T is the absolute temperature, and R is the gas constant. The actual M_c and X_c calculated using Eq. (7) are also listed in Table 7. The crosslink density can be used as a factor in determining the difference in the physical properties of each cured film. A higher crosslink density leads to better physical performance.

The T_g of WPCU-L800-1MA, WPCU-L800-Si-1MA, WPCU-L800-3A and WPCU-L800-Si-3A was 44.5 °C, 53.7 °C, 62.2 °C and 89.0 °C, respectively. All UV-cured samples showed a single T_g, which result from the good miscibility between the hard and soft segments as well as the complete phase mixing of polyurethane [40,42]. The T_g of the cured films end-capped with tri-acrylate (WPCU-L800-3A and WPCU-L800-Si-3A) were higher than monomethacrylate end-capped samples (WPCU-L800-1MA and WPCU-L800-Si-1MA) owing to the former's higher functionality, which produced a network structure with a higher crosslink density. This can be confirmed by the theoretical and actual M_c and X_c. There were some differences between methods but the order of the crosslink density was as follows: WPCU-L800-1MA < WPCU-L800-Si-1MA < WPCU-L800-3A < WPCU-L800-Si-3A.

The T_g and crosslink density increased with increasing functionality of the end-capping groups because the curing rate and final conversion of the sample with higher functionality was high and a denser film network was made. Generally, the introduction of soft

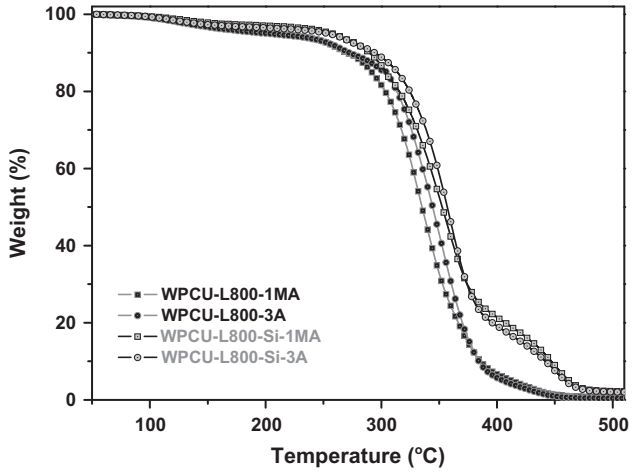

(a) Weight loss curves

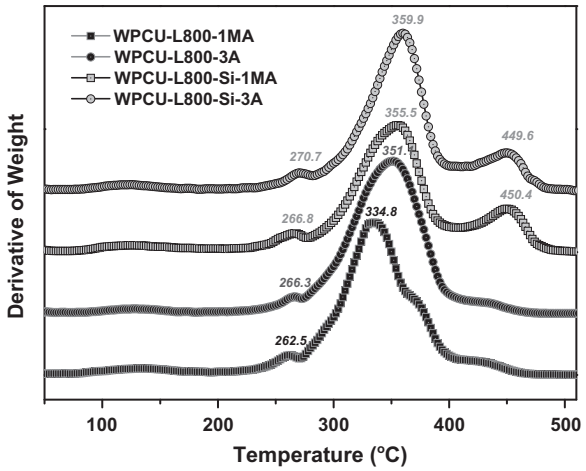

(b) Derivative of weight loss curve

Fig. 7. Thermogravimetric analysis of the UV-cured film of PDMS-modified polycarbonate-based polyurethane (meth)acrylate dispersions. (a) Weight loss curve, (b) derivative of weight loss curve.

PDMS segments is expected to decrease the T_g of the matrix [14]. However, the effect of PDMS incorporation was positive on the T_g and crosslink density. The molecular weight between (M_c) of UV-cured sample with PDMS decreased because the molecular weight of PDMS (550 g/mol) was lower than that of PCDL (800 g/mol). These results were also related to the final conversion of the C=C double bonds by photo-DSC. In the case of PDMS with mono-methacrylate end-capping, PDMS improved the chain flexibility and increased the final conversion, which led to increasing T_g and crosslink density. On the other hand, there was a contradicting effect on PDMS with the tri-acrylate end-capping sample. Decreasing the final conversion due to the steric hindrance of PDMS lead to a decrease in T_g and

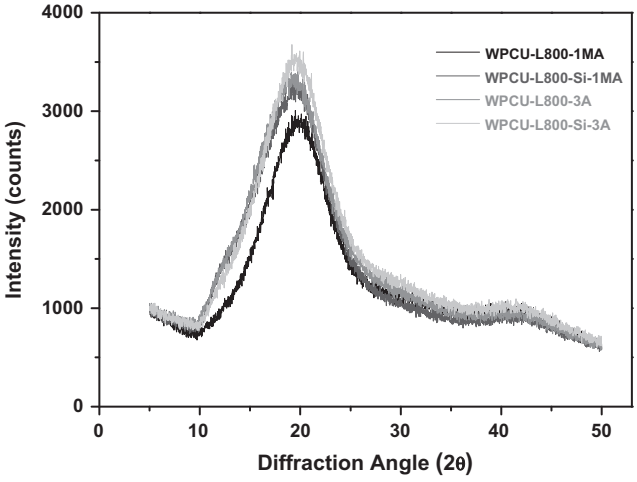

Fig. 8. X-ray diffraction patterns of the UV-cured film of PDMS-modified polycarbonate-based polyurethane (meth)acrylate dispersions.

the crosslink density. However, the lower molecular weight of PDMS than that of PCDL led to an increase in T_g and crosslink density. Judging from the actual T_g and crosslink density of PDMS with tri-acrylate end-capping, the latter factor had a stronger effect on the T_g and crosslink density than the former factor.

3.5. Tensile strength

Tensile test is carried out to investigate the basic mechanical properties of the modulus, maximum tensile strength, elongation at break and toughness of the polymeric materials [27]. Fig. 6 presents the effects of the functionality and PDMS on the tensile behavior, such as the strain–stress behavior (a) and the maximum tensile strength and elongation at break (b).

The effects of the functionality on the tensile behaviors were different from those of the incorporation of PDMS. WPCU-L800-Si-1MA and WPCU-L800-Si-3A had a tensile strength of 14.3 MPa and 32.9 MPa with their percent elongation of 144% and 55.9%, respectively. WPCU-L800-Si-3A showed a very high initial modulus and maximum tensile strength but a lower elongation at break. Generally, there is some trade-off between the strain properties and tensile strength [15]. On the other hand, WPCU-L800-1MA and WPCU-L800-3A had a tensile strength of 8.3 MPa and 18.6 MPa with their percent elongation of 220% and 268%, respectively. WPCU-L800-3A showed a very high initial modulus and maximum tensile strength as well as very high elongation at break. This was attributed to the higher functionality leading higher conversion and forming tougher films with a high crosslink density.

3.6. Thermal property

An investigation of the thermal degradation process provides methods for the determining optimum conditions for manipulat-

Table 8
Characteristic thermal decomposition data of the UV-cured film of PDMS-modified polycarbonate-based polyurethane (meth)acrylate dispersions.

Samples	Weight			Peaks of deriv. weight (°C)		
	$T_{10\%}$ (°C)	$T_{50\%}$ (°C)	wt% at 500 °C	First	Second	Third
WPCU-L800-1MA	270.3	335.3	0.75	262.5	334.8	–
WPCU-L800-3A	271.9	344.4	0.43	266.3	351.1	–
WPCU-L800-Si-1MA	289.8	352.6	2.26	266.8	355.5	450.4
WPCU-L800-Si-3A	294.5	357.0	2.08	270.7	359.9	449.6

$T_{10\%}$: 10 wt% loss temperature, $T_{50\%}$: 50 wt% loss temperature.

ing and processing the polymer as well as obtaining high performance polymers with improved thermal stability [10]. In addition, accelerating the lifetime testing of polymers can be possible by short-term experiments used to predict the in-use lifetime through thermogravimetric analysis [40]. Fig. 7 shows the thermal stability of the UV-cured films at temperatures ranging from 30 °C to 600 °C. Fig. 7a and b shows the weight loss curves and derivative of the weight profiles of each sample, respectively. Table 8 lists the characteristic thermal decomposition data of each cured sample. The maximum thermal degradation peak temperatures of the first, second and third step are also listed in Table 8 [39].

The UV-cured films without PDMS (WPCU-L800-1MA, WPCU-L800-3A) were decomposed in two steps. The first part of degradation correlates with the hard segment (IPDI–DMPA–HEMA or IPDI–DMPA–PETA segment) of the polyurethane chain, and the second peak indicates degradation of the soft segment (PCDL) [43,44]. The maximum thermal degradation of the hard and soft segment of polyurethane occurred at 260–270 °C and 335–360 °C, respectively.

However, the UV-cured films with PDMS (WPCU-L800-Si-1MA, WPCU-L800-Si-3A) had three decomposition peaks. The first and second peaks were for the hard and soft segment, respectively, as mentioned above. The third peak reflects the inorganic siloxane of the PDMS segment. The maximum thermal decomposition of the PDMS chains occurred at approximately 450 °C. Incorporation of PDMS increased the thermal stability of polyurethane (meth)acrylate dispersion due to the greater thermal stability of PDMS component [26]. On the other hand, increasing the functionality of the end-capping group improved the thermal stability slightly by 5–17 °C in the first and second degradation peaks. This is because higher functionality form networks with a high crosslink density, which improves the thermal stability of the UV-cured films.

3.7. X-ray diffraction

WAXD was performed to investigate the underlying microstructure of the UV-cured films [45]. Fig. 8 shows wide angle WAXD of each UV-cured film. The XRD patterns of all samples were similar with a large wide diffraction halo at around 20° and a small wide diffraction halo at around 42°. This means that the microstructures of all samples was amorphous since the molecular chain distance of non-crystalline materials is approximately 0.4–0.5 nm [16,45]. The hard segment regions in the polyurethane were difficult to crystallize owing to the flexibility of the PDMS and polycarbonate segment, even though the UV-cured film had a crosslinked structure. In addition, the molecular chain of polycarbonate was insufficient for chain folding and to form a crystalline structure [46]. There were some differences in the intensity between samples, and the order of the intensity was as follows: WPCU-L800-1MA < WPCU-L800-Si-1MA < WPCU-L800-3A < WPCU-L800-Si-3A.

4. Conclusions

UV-curable polycarbonate-based polyurethane dispersions were modified by the incorporation of a hydroxy-terminated PDMS into the soft segments to improve the thermal properties and control the surface properties. The effect of functionality with or without PDMS on the properties was investigated by end-capping with 2-HEMA or PETA. The UV-curing behavior depended mainly on the functionality, irrespective of the incorporation PDMS. The surface free energy of the UV-cured film containing PDMS was low and the thermal stability was improved. T_g and crosslink density increased with the incorporation of PDMS and increasing functionality, which resulted in improved physical properties such as tensile strength. Consequently, waterborne UV-curable coatings with PDMS and high functionality showed improved thermal and physical properties with a low surface energy.

Acknowledgements

This study was supported partially by Industrial Strategic Technology Development Program (10035163) – "Development of highly flexible pre-finished color metal sheet and modular process technology for automotive", Ministry of Knowledge and Economy, Republic of Korea.

References

[1] B. Műller, U. Poth, Coatings Formulation, Vincentz, Hannover, 2006.
[2] M. Nanea, High Solid Binders, Vincentz Network, Hannover, 2008.
[3] C.Y. Bai, X.Y. Zhang, J.B. Dai, Prog. Org. Coat. 60 (2007) 63–68.
[4] J.S.J. Pruskowski, Waterborne Coatings Technology, Federation of Societies for Coatings Technology, Blue Bell, PA, 2004.
[5] P. Glöckner, T. Jung, S. Struck, K. Studer, Radiation Curing – Coatings and Printing Inks, Vincentz Network, Hannover, 2008.
[6] H.-D. Hwang, J.-I. Moon, J.-H. Choi, H.-J. Kim, S.D. Kim, J.C. Park, J. Ind. Eng. Chem. 15 (2009) 381–387.
[7] R. Schwalm, UV Coatings: Basics, Recent Developments and New Applications, Elsevier, Amsterdam; London, 2007.
[8] R. Schwalm, L. Haussling, W. Reich, E. Beck, P. Enenkel, K. Menzel, Prog. Org. Coat. 32 (1997) 191–196.
[9] S.A. Madbouly, J.U. Otaigbe, Prog. Polym. Sci. 34 (2009) 1283–1332.
[10] D.K. Chattopadhyay, D.C. Webster, Prog. Polym. Sci. 34 (2009) 1068–1133.
[11] Q.Z. Zhu, S.Y. Feng, C. Zhang, J. Appl. Polym. Sci. 90 (2003) 310–315.
[12] A. Stanciu, V. Bulacovschi, S. Oprea, S. Vlad, Polym. Degrad. Stabil. 72 (2001) 551–558.
[13] B.U. Ahn, S.K. Lee, S.K. Lee, J.H. Park, B.K. Kim, Prog. Org. Coat. 62 (2008) 258–264.
[14] S.K. Rath, J.G. Chavan, S. Sasane, A. Srivastava, M. Patri, A.B. Samui, B.C. Chakraborty, S.N. Sawant, Prog. Org. Coat. 65 (2009) 366–374.
[15] C.Y. Bai, X.Y. Zhang, J.B. Dai, J. Macromol. Sci. A 44 (2007) 1203–1208.
[16] C.Y. Bai, X.Y. Zhang, J.B. Dai, J.H. Wang, J. Coat. Technol. Res. 5 (2008) 251–257.
[17] U. Meier-Westhues, Polyurethanes: Coatings, Adhesives and Sealants, Vincentz Network, Hannover, 2007.
[18] S. Nakano, Prog. Org. Coat. 35 (1999) 141–151.
[19] T. Masubuchi, H. Fukumura, H. Masuhara, K. Suzuki, N. Hayashi, J. Photochim. Photobiol. A 145 (2001) 215–222.
[20] M. Furukawa, Y. Hamada, K. Kojio, J. Polym. Sci. Pol. Phys. 41 (2003) 2355–2364.
[21] K. Kojio, Y. Nonaka, T. Masubuchi, M. Furukawa, J. Polym. Sci. Pol. Phys. 42 (2004) 4448–4458.
[22] M. Gindl, G. Sinn, W. Gindl, A. Reiterer, S. Tschegg, Colloid Surf. A 181 (2001) 279–287.
[23] B.K. Kim, J.S. Yang, S.M. Yoo, J.S. Lee, Colloid Polym. Sci. 281 (2003) 461–468.
[24] B.K. Kim, B.U. Ahn, M.H. Lee, S.K. Lee, Prog. Org. Coat. 55 (2006) 194–200.
[25] S.K. Lee, B.K. Kim, J. Colloid Interf. Sci. 336 (2009) 208–214.
[26] C.Y. Bai, X.Y. Zhang, J.B. Dai, W.H. Li, Chinese Chem. Lett. 17 (2006) 369–372.
[27] F. Levine, J. La Scala, W. Kosik, Prog. Org. Coat. 69 (2010) 63–72.
[28] H.Y. Choi, C.Y. Bae, B.K. Kim, Prog. Org. Coat. 68 (2010) 356–362.
[29] T. Su, G.Y. Wang, S.L. Wang, C.P. Hu, Eur. Polym. J. 46 (2010) 472–483.
[30] A. Palanisamy, Prog. Org. Coat. 60 (2007) 161–169.
[31] Q. Yu, S. Nauman, J.P. Santerre, S. Zhu, J. Appl. Polym. Sci. 82 (2001) 1107–1117.
[32] K.S. Anseth, C.N. Bowman, N.A. Peppas, J. Polym. Sci. Pol. Chem. 32 (1994) 139–147.
[33] X.S. Jiang, H.J. Xu, H. Yin, Polymer 45 (2004) 133–140.
[34] R.J. Good, J. Adhes. Sci. Technol. 6 (1992) 1269–1302.
[35] Y.K. Lee, H.J. Kim, M. Rafailovich, J. Sokolov, Int. J. Adhes. Adhes. 22 (2002) 375–384.
[36] J.W. Wang, L.P. Wang, J. Fluorine Chem. 127 (2006) 287–290.
[37] M.J. Geerken, R.G.H. Lammertink, M. Wessling, Colloid Surf. A 292 (2007) 224–235.
[38] J.B. Dai, X.Y. Zhang, J. Chao, C.Y. Bai, J. Coat. Technol. Res. 4 (2007) 283–288.
[39] A.K. Mishra, R.S. Mishra, R. Narayan, K.V.S.N. Raju, Prog. Org. Coat. 67 (2010) 405–413.
[40] A. Asif, W.F. Shi, X.F. Shen, K.M. Nie, Polymer 46 (2005) 11066–11078.
[41] U.W. Gedde, Polymer Physics, Kluwer Academic Publishers, Dordrecht, 1995.
[42] Y.U. Ahn, S.K. Lee, S.K. Lee, H.M. Jeong, B.K. Kim, Prog. Org. Coat. 60 (2007) 17–23.
[43] J.W. Yang, Z.M. Wang, Z.H. Zeng, Y.L. Chen, J. Appl. Polym. Sci. 84 (2002) 1818–1831.
[44] A. Asif, W.F. Shi, Polym. Adv. Technol. 15 (2004) 669–675.
[45] J.W. Xu, W.F. Shi, W.M. Pang, Polymer 47 (2006) 457–465.
[46] T. Zhang, W.J. Wu, X.J. Wang, Y.P. Mu, Prog. Org. Coat. 68 (2010) 201–207.